VOL. 15, NO. 18, SEPTEMBER 2020 ISSN 1819-6608
ARPN Journal of Engineering and Applied Sciences

www.arpnjournals.com

CLASSICAL AND ADVANCED CONTROL APPLIED TO A NON-LINEAR SYSTEM OF COUPLED TANKS

Diego F. Escobar-Núñez, Henry Ortiz-Otálora and Diego F. Sendoya-Losada
Department of Electronic Engineering, Faculty of Engineering, Surcolombiana University, Neiva, Huila, Colombia
E-Mail: diego.sendoya@usco.edu.co

ABSTRACT

In this work two model-based controllers have been designed in order to regulate a non-linear system of coupled tanks. First, a Proportional-Integral-Derivative (PID) controller was designed. This algorithm requires a linear model, so the model was linearized around a certain equilibrium point. Secondly, Internal Model Controller (IMC) was designed. Finally, the performance of the controllers is evaluated, in order to carry out a tracking to a reference level and an effective rejection of the disturbances.

Keywords: IMC, Level control, PID, RMSE.

1. INTRODUCTION

In almost all the applications of industrial processes, the control of the variables is critical for the safe and efficient operation of the same. The most common controlled variables are pressure, level, temperature, and flow. Level control loops are very common in the industry; in fact, they occupy the second place after the flow control loops. Due to the importance and the large number of processes that require a precise level control, the Surcolombiana University recently acquired a tank system called CE105 MV. As can be seen in Figure-1, this system presents a configuration similar to that which can be found in many industrial applications or as part of a much larger and more sophisticated plant.

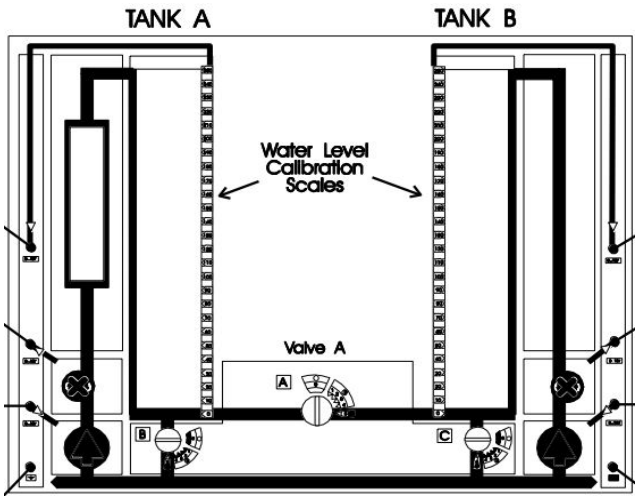

Figure-1. CE105MV System.

Usually the control of the liquid level in a tanks system is done by classical control techniques such as PI or PID, due to its well-known and simple structure [1]–[3]. For the design of these conventional controllers it is necessary to choose a setpoint and then to find a linear model of the system, ensuring that the control works well in this region, but when it moves away from the setpoint, the controller loses effectiveness [4]–[5]. In this contribution, Internal Model Control (IMC) is applied to a coupled tank system - CE105 MV [6]. For this paper, a Single-Input Single-Output (SISO) system configuration has been considered. The input voltage is applied to the pump of tank A and the output liquid level is measured in tank B.

There are many papers about liquid level control using classical or advanced control techniques [7]–[13]. In this contribution, the Proportional-Integral-Derivative (PID) controller is used, in order to carry out a tracking to a reference level and an effective rejection of the disturbances. Then a comparison with the Internal Model Control (IMC) algorithm is done. The performance of these controllers is tested and evaluated in a simulation environment. The simulation is done using the Matlab®/Simulink® software.

2. MATERIALS AND METHODS

2.1 Process Model

The presented mathematical model is given by the equations that describe the complete system. Figure-2 shows their respective schematic. The dynamic model is determined by the relationship between the inlet flow Q_i and the outlet flow Q_c through the discharge valve. Equation (1) describes this relationship.

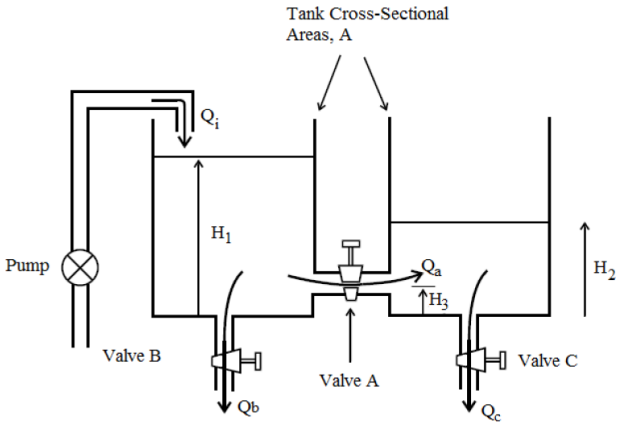

Figure-2. Schematic of coupled tanks.

$$Q_i - Q_a - Q_b = A\frac{dH_1}{dt} \quad (1)$$

$$Q_a - Q_c = A\frac{dH_2}{dt} \quad (2)$$

Valves are assumed to behave as a standard sharp-edged port [14], and the outflow through the discharge valve is related to the level of liquid in the tank by Equations (3), (4), and (5):

$$Q_a = aC_a\sqrt{2g(H_1 - H_2)} \quad (3)$$

$$Q_b = aC_b\sqrt{2gH_1} \quad (4)$$

$$Q_c = aC_c\sqrt{2gH_2} \quad (5)$$

A is the cross-sectional area of the tanks; a is the cross-sectional area of the valve orifice;C_a, C_b, and $C_c$are the discharge coefficients of the valves and g is the gravity constant. Combining Equations (1) to (5) gives:

$$Q_i = A\frac{dH_1}{dt} + aC_a\sqrt{2g(H_1 - H_2)} + aC_b\sqrt{2gH_1} \quad (6)$$

$$A\frac{dH_2}{dt} = aC_a\sqrt{2g(H_1 - H_2)} - aC_c\sqrt{2gH_2} \quad (7)$$

Equations (6) and (7) are first order nonlinear differential equations, to be useful in control systems, the equations must be linearized considering small variations on the desired operating fluid level in the tanks [8]. Applying the Taylor series and performing the Laplace transform, the transfer function of the system for coupled tanks is obtained:

$$G(s) = \frac{D_1}{s^2 + D_2 s + D_3} \quad (8)$$

Where:

$$D_1 = \frac{K_p C_a a\sqrt{2g}}{4A^2\sqrt{H_1 - H_2}}$$

$$D_2 = \frac{a\sqrt{2g}}{A}\left(\frac{C_b}{2\sqrt{H_1}} + \frac{C_a}{H'} + \frac{C_c}{2\sqrt{H_2}}\right)$$

$$D_3 = \frac{a^2 2g}{4A^2}\left(\frac{C_b C_a}{H'\sqrt{H_1}} + \frac{C_b C_c}{\sqrt{H_1}\sqrt{H_2}} + \frac{C_c C_a}{H'\sqrt{H_2}}\right)$$

$$H' = \sqrt{H_1 - H_2}$$

Although the water enters the tank from the bottom, the dimensions of the system are small enough so that no delay in the change of level is observed. The values of the system parameters are shown in Table-1.

Table-1. System parameters [15].

Symbol	Description	Value
A	Cross-sectional area of the tanks	$9350\text{x}10^{-6}\text{m}^2$
a	Cross-sectional area of the valve orifice	$78.50\text{x}10^{-6}\text{m}^2$
C_a	Discharge coefficient of valve A	0.5
C_b	Discharge coefficient of valve B	0.2
C_c	Discharge coefficient of valve C	0.2
h_{max}	Maximum liquid level	0.25 m
v_{max}	Maximum input voltage	10 V
K_p	Pump gain	$6.66\text{x}10^{-6}\text{m}^3/\text{sV}$
K_h	Sensor level gain	$40\ \text{V/m}$
g	Gravity constant	$9.8\ \text{m/s}^2$

The non-linear dynamics (6) and (7) must be linearized before PID and IMC control can be applied. The linearization was made using the first order Taylor expansion around the equilibrium point $h^* = 0.1$ m. For the equilibrium point: $f(v_i^*, h^*) = 0$. Linearizing the coupled tanks dynamics yields the following transfer function:

$$G(s) = \frac{2.616\times10^{-5}}{s^2 + 0.1695s + 0.001793} \quad (9)$$

2.2 PID Controller

The "textbook" algorithm that describes the behavior of the PID controller is presented in (10):

$$u(t) = K_p\left[e(t) + \frac{1}{T_i}\int_0^t e(\tau)d\tau + T_d\frac{de(t)}{dt}\right] \quad (10)$$

$u(t)$ is the output signal of the PID controller, which in this case corresponds to the voltage applied to the pump. $e(t)$ is the input signal of the PID controller, which is defined as $e(t) = r(t) - y(t)$, where $r(t)$ is the setpoint and $y(t)$ is the output of the process, that is, the level of liquid in the tank. K_p is the proportional gain,T_i is the integrationtime, and T_d is the differentiation time.

Applying the Laplace transform to (10), the transfer function of the PID controller is found:

$$\frac{U(s)}{E(s)} = K_p\left[1 + \frac{1}{T_i s} + T_d s\right] \quad (11)$$

However, the practical implementation form is given by:

$$\frac{U(s)}{E(s)} = K_p\left[1 + \frac{1}{T_i s} + \frac{T_d s}{1 + \alpha T_d s}\right] \quad (12)$$

Therefore, the transfer function for the practical PID controller, which gives minimum overshoot and minimum settling time, is:

$$\frac{U(s)}{E(s)} = 80.9781 + \frac{0.8756}{s} + \frac{14.7392s}{s+0.0274} \quad (13)$$

2.3 IMC

An IMC controller presents the structure of Figure-3.

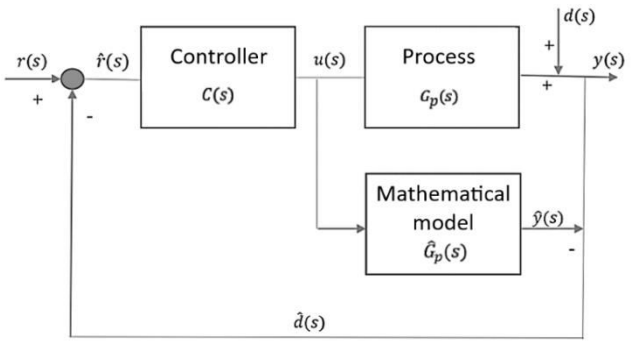

Figure-3. Schematic of an IMC.

The IMC structure has a mathematical model $\hat{G}_p(s)$ in parallel to the plant $G_p(s)$ with the same input $u(s)$ producing an output $\hat{y}(s)$, which will be subtracted from the output $y(s)$ of the plant obtaining a signal $\hat{d}(s)$. This is fed backand compared to the required parameter $r(s)$ to supply the controller $C(s)$ using the signal $\hat{r}(s)$.

Commonly, the IMC defines its bases in the inverse use of the mathematical model of the process, with the aim of obtaining robust control [16]-[17]. In this way the differences between the real plant $G_p(s)$ and its approximate mathematical model $\hat{G}_p(s)$ (9) are reduced. In addition, non-measurable disturbances are monitored.

If $G_P(s) = \hat{G}_p(s)$ and $d(s) = 0$, both the input voltage and the non-measurable disturbances considered in the design will return to the controller by means of feedback generating permanent control of the system.

The following equations describe the IMC controller in Figure-3.

$$\mathrm{y(s) = G_p(s)u(s) + d(s)} \quad (14)$$

$$\mathrm{\hat{y}(s) = \hat{G}_p(s)u(s)} \quad (15)$$

$$\mathrm{\hat{d}(s) = y(s) - \hat{y}(s) + d(s)} \quad (16)$$

$$\mathrm{\hat{r}(s) = r(s) - \hat{d}(s)} \quad (17)$$

With $y(s) = G_p(s)u(s)$, $u(s) = \hat{r}(s)C(s)$, and taking into account the disturbances, the output can be expressed as follows:

$$\mathrm{y(s) = G_p(s)C(s)r(s)} \quad (18)$$

To achieve zero steady-state error, the condition $y(s) = r(s)$ must be met. When approached by means of (14) the multiplication between $G_p(s)$ and $C(s)$ must be equal to one. To obtain the function that satisfies this product, $C(s)$ must be equal to the inverse of the plant, as shown below:

$$\mathrm{C(s) = \frac{1}{G_p(s)} = G_p(s)^{-1}} \quad (19)$$

By inverting the plant model (9), the controller required by the IMC model is obtained:

$$\mathrm{C(s) = \frac{s^2+0.1695s+0.001793}{2.616\times10^{-5}}} \quad (20)$$

The transfer function of the controller must be its proper or semi-proper, that is, the degree of the denominator must be greater than or equal to the degree of the numerator, respectively. From the new configuration obtained (18), it is possible to deduce that it is an improper function, for this reason, the implementation of the filter $f(s)$ is carried out:

$$\mathrm{f(s) = \frac{1}{(\lambda s+1)^n}} \quad (21)$$

n is selected, so that when multiplied with $C(s)$ a semi-proper or proper function is obtained. λ is a closed-loop response speed tunning parameter, with a small value for a fast system response and a large value for a slowdown.

For the choice of parameters, the intrinsic physical characteristics of the function plant are considered (9). In which the values $n = 2$ and $\lambda = 25.5$ are obtained.

$$\mathrm{f(s) = \frac{1}{(25.5s+1)^2}} \quad (22)$$

The filter converts equation (19) into a semi-proper function as follows:

$$\mathrm{C(s) = f(s)\hat{G}_p(s)^{-1}} \quad (23)$$

$$\mathrm{C(s) = \left(\frac{s^2 + 0.1695s + 0.001793}{2.616 \times 10^{-5}}\right)\left(\frac{1}{(25.5s+1)^2}\right)}$$

Therefore, from (18), the closed-loop response of the system is:

$$\mathrm{y(s) = \left(\frac{1}{(\lambda s+1)^n}\right) r(s) = \left(\frac{1}{(25.5s+1)^2}\right) r(s)} \quad (24)$$

3. RESULTS AND DISCUSSIONS

The simulation was conducted towards two scenarios to compare the behavior of the PID and IMC algorithms. The performance of the controllers is evaluated, in order to carry out a tracking to a reference level and an effective rejection of the disturbances.

3.1 Scenario 1: Disturbance Rejection

In order to evaluate the performance of the controlled system when a disturbance is applied, the setpoint is fixed at 0.1 m. After the response reaches the steady state a disturbance is applied to the system, which consists of a change in the discharge coefficient of valve C, that is, C_c goes from 0.2 to 0.4. Finally, when the response reaches the setpoint again, the discharge coefficient is changed from 0.4 to 0.2. Figure-4 shows the output level when PID and IMC algorithms are used.

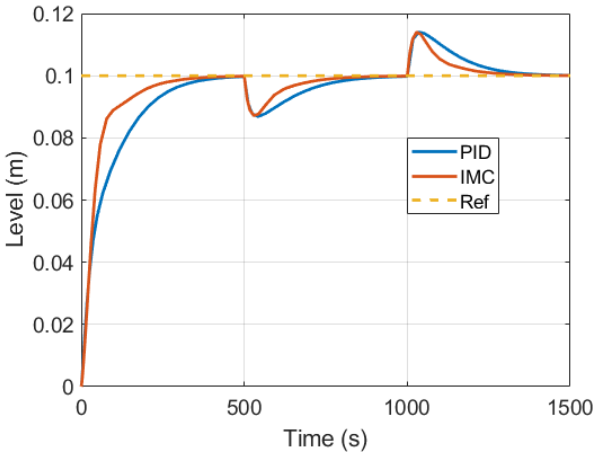

Figure-4. Disturbance rejection with PID and IMC.

Initially the response does not present overshoot in both cases. When the system stabilizes the discharge coefficient of valve C is changed from 0.2 to 0.4, this disturbs the system because the outflow increases. At 500 seconds the output level of the system is reduced due to this situation. However, the controllers increase the control effort (as can be observed in Figure-5) to compensate for the reduction in the output level and increase it again to 0.1 m. When IMC algorithm is used, the change in the output level of the system is less.

Finally, at 1000 seconds, the discharge coefficient of valve C is changed from 0.4 to 0.2. Because of this generates a reduction in the output flow, it is observed how the output level increases when PID acts. Again, this change is less when IMC in used. Both controllers adjust the voltage applied to the system to compensate for the increase in level. The output stabilizes again at 0.1 m, showing the robustness of the controllers against changes in the process parameters.

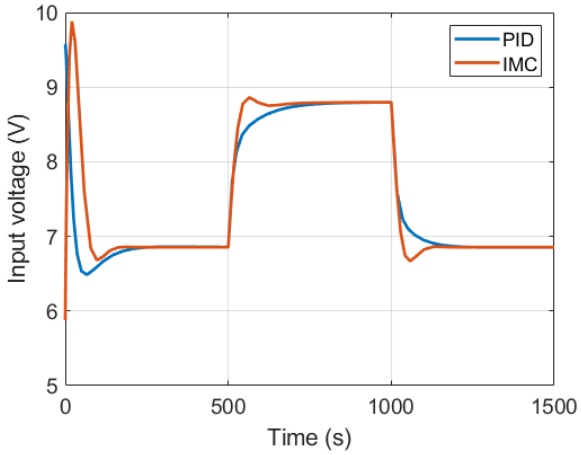

Figure-5. Input voltage for disturbance rejection.

3.2 Scenario 2: Setpoint Tracking

In order to evaluate how the system behaves in closed loop at different points of operation, a reference signal composed of 4 steps with amplitudes of 0.04, 0.08, 0.12, and 0.16 m is applied. Figure-6 shows how the process output $y(t)$ tracks a setpoint.

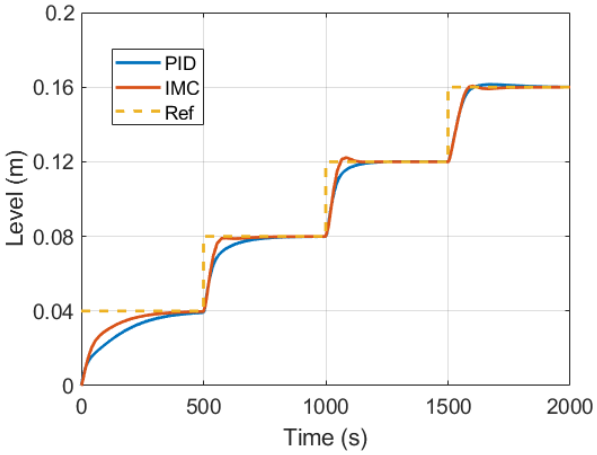

Figure-6. Setpoint tracking with PID and IMC.

For both controllers, the model is linearized in a point corresponding with an output level $h^* = 0.1$ m. As can be observed, the response is better for the last steps. But as soon as the setpoint lies a bit further, results worse fast, for instance, the first setpoint step shows a longer settling time. As soon as the setpoint comes in a value close to 10 cm, the controller starts giving good results. It can be seen that IMC gives very good results. The output follows the set point changes with very little overshoot and less settling time.

Finally, Figure-7 shows the control effort for both controllers.

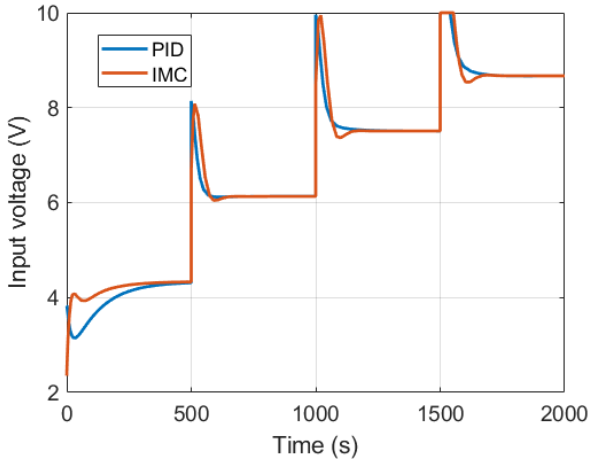

Figure-7. Input voltage for setpoint tracking.

In order to obtain a detailed results analysis of the comparative study between the PID and IMC algorithms, the Root Mean Square Error (RMSE) variations were used.

$$RMSE = \sqrt{\frac{\sum_{t=1}^{N}[r(t)-y(t)]^2}{N}} \quad (25)$$

where $r(t)$ is the setpoint signal, $y(t)$ is the output signal, and N is the number of samples. Table-2 shows the RMSE variations for both the PID algorithm and the IMC algorithm when the two simulation scenarios are applied.

Table-2. RMSE variations for PID and IMC.

Scenario	PID (%)	IMC (%)
1	19.21	16.96
2	14.22	12.97

The implemented IMC algorithm presents a better behavior in the two scenarios compared to the PID algorithm.

Although the computational cost of the implementation of the IMC algorithm is higher, the system response is noticeably faster than when the PID algorithm is used. This can be an advantage in systems where it is necessary to minimize the values of overshoot and settling time. However, for processes where these requirements are not necessary, the PID algorithm would be more viable because of its simplicity of implementation.

4. CONCLUSIONS

In this work, the performance of PID and IMC algorithms was evaluated. It can be observed that the IMC is more effective in rejecting disturbances. This is because it uses a greater control effort when there are changes in the system parameters. In the same way, because the IMC the tracking to the variations in the reference level is much better. In addition, as the model used is more precise, the control effort required is greater when changing from one setpoint to another.

REFERENCES

[1] J. F. Caipa-Roldán, J. M. Salamanca and J. L. Rodríguez-Herrera. 2010. Control digital de nivel para sistema de tanques interconectados mediante servo-válvula. Ingeniería Investigación y Desarrollo. 10(1): 55-63.

[2] E. Govinda-Kumar and J. Arunshankar. 2018. Control of nonlinear two-tank hybrid system using sliding mode controller with fractional-order PI-D sliding surface. Computers & Electrical Engineering. 71: 953-965.

[3] V. Bhambhani and Y. Q. Chen. 2008. Experimental study of fractional order proportional integral (FOPI) controller for water level control. 47th IEEE Conference on Decision and Control.

[4] A. Başçi and A. Derdiyok. 2016. Implementation of an adaptive fuzzy compensator for coupled tank liquid level control system. Measurement. 91: 12-18.

[5] S. R. Mahapatro. 2014. Control algorithms for a two tank liquid level system: An experimental study. Diss.

[6] D. F. Sendoya-Losada, D. C. Vargas-Duque and I. J. Ávila-Plazas. 2018. Implementation of a neural control system based on PI control for a non-linear process. 1st IEEE Colombian Conference on Applications in Computational Intelligence.

[7] S. Banerjee, S. Das, S. Khatua, A. Gupta, P. Arvind, S. Kumari and S. Das. 2017. Liquid level control system using observer based constrained discrete-time model predictive control. IEEE International Conference on Circuit, Power and Computing Technologies (ICCPCT). pp. 1-8.

[8] A. Shehu and N. A. Wahab. 2016. Applications of MPC and PI controls for liquid level control in coupled-tank systems. IEEE International Conference on Automatic Control and Intelligent Systems (I2CACIS). pp. 119-124.

[9] M. Dulău and T. M. Dulău. 2016. Multivariable system with level control. Procedia Technology. 22: 614-622.

[10] P. Gondaliya and M. C. Patel. 2015. Design and implementation of model predictive control for a liquid level system using LabVIEW. International Journal for Scientific Research & Development. 3(6): 1313-1316.

[11] M. Essahafi. 2014. Model predictive control (MPC) applied to couple tank liquid level system. arXiv preprint arXiv: 1404.1498.

[12] M. U. Khalid and M. D. Kadri. 2012. Liquid level control of nonlinear coupled tanks system using linear model predictive control. IEEE International Conference on Emerging Technologies (ICET). pp. 1-5.

[13] Currie and D. I. Wilson. 2010. Lightweight model predictive control intended for embedded applications. IFAC Proceedings. 43(5): 278-283.

[14] Ogata Katsuhito, Dinamica de sistemas, Prentice Hall, Mexico, 1987.

[15] Tec Quipment. 2016. CE105 and CE105MV Coupled Tanks user manual. TecQuipment Ltd.

[16] R. De Keyser. Internal Model Control: IMC. Ghent University.

[17] B. W. Wayne-Bequette Process Control: Modeling, Design, and Simulation, primeraedición, Prentice Hall PTR. 2002, pp. 330-336.

[18] D.F. Sendoya-Losada, J.D Quintero-Polanco. 2018. Control of yaw angle in a miniature helicopter. ARPN Journal of Engineering and Applied Sciences. 13(2): 620-626.

[19] D. F. Sendoya-Losada, J.D Quintero-Polanco. 2018. PID controller applied to an unmanned aerial vehicle. ARPN Journal of Engineering and Applied Sciences. 13(1): 325-334.

[20] D. F. Sendoya-Losada, J.D Quintero-Polanco. 2018. Design and validation of a PID auto-tuning algorithm. ARPN Journal of Engineering and Applied Sciences. 13(11): 3797-3802.

[21] D. F. Sendoya-Losada. 2018. KCR PID auto-tuner algorithm applied to a FOT device. ARPN Journal of Engineering and Applied Sciences. 13(7): 2505-2510.